

# Extraction of the species dependent dipole moment from high-order harmonic spectra in rare gas atoms

Anh-Thu Le,<sup>1</sup> Toru Morishita,<sup>1,2</sup> and C. D. Lin<sup>1</sup>

<sup>1</sup>*Department of Physics, Cardwell Hall, Kansas State University, Manhattan, KS 66506, USA*

<sup>2</sup>*Department of Applied Physics and Chemistry, University of Electro-Communications,  
1-5-1 Chofu-ga-oka, Chofu-shi, Tokyo, 182-8585, Japan and PRESTO,  
Japan Science and Technology Agency, Kawaguchi, Saitama 332-0012, Japan*

(Dated: February 2, 2008)

Based on high-order harmonic generation (HHG) spectra obtained from solving the time-dependent Schrödinger equation for atoms, we established quantitatively that the HHG yield can be expressed as the product of a returning electron wave packet and the photo-recombination cross sections, and the shape of the returning wave packet is shown to be largely independent of the species. By comparing the HHG spectra generated from different targets under identical laser pulses, accurate structural information, including the phase of the recombination amplitude, can be retrieved. This result opens up the possibility of studying the target structure of complex systems, including their time evolution, from the HHG spectra generated by short laser pulses.

PACS numbers: 42.65.Ky, 33.80.Rv

When an atom is subjected to a strong driving laser field, one of the most important nonlinear response processes is the generation of high-order harmonics. In the past decade, high-order harmonic generation (HHG) has been used for the production of single attosecond pulses [1, 2, 3] and attosecond pulse trains [4], thus opening up new opportunities for attosecond time-resolved spectroscopy. HHG is understood using the three-step model (TSM) [5, 6, 7] – first the electron is released by tunnel ionization; second, it is accelerated by the oscillating electric field of the laser and later driven back to the target ion; and third, the electron recombines with the ion to emit a high energy photon. A semiclassical formulation of the TSM based on the strong-field approximation (SFA) is given by Lewenstein *et al* [7]. In this model (often called Lewenstein model), the liberated continuum electron experiences the full effect from the laser field, but not from the ion that it has left behind. In spite of this limitation, the SFA model has been used quite successfully, in particular, for analysis of the attosecond synchronization of high harmonics, see Mairesse *et al* [8] and references therein. However, since the continuum electron recombines when it is near the parent ion, the neglect of electron-ion interaction in the SFA model is rather questionable.

According to the TSM, the last step of HHG is analogous to the radiative recombination process in electron-ion collisions. Thus one may write the HHG signal as

$$S(\omega) = W(E) \times |d(\omega)|^2 \quad (1)$$

where  $d(\omega)$  is the photo-recombination (PR) transition dipole and  $W(E)$  is the returning “electron wave packet”. Electron energy  $E$  is related to the emitted photon energy  $\omega$  by  $E = \omega - I_p$ , with  $I_p$  being the ionization potential of the target. Clearly the HHG signal  $S(\omega)$  and  $W(E)$  depend on the laser properties. On the other hand,  $d(\omega)$

is the property of the target only. The factorization in Eq. (1) is most useful when one compares the HHG spectra from two different targets in the identical laser field. Assuming that the shape of  $W(E)$  is species independent, by measuring the relative HHG yields, one can deduce the PR cross section of one species if the PR cross section of the other is known. The validity of Eq. (1) has been shown recently in Morishita *et al.* [9] using HHG spectra calculated by solving the time-dependent Schrödinger equation (TDSE) for atoms. The validity of this factorization has also been shown for rare gas atoms by Levesque *et al.* [10] and for N<sub>2</sub> and O<sub>2</sub> molecules [11], where the HHG spectra were calculated using the SFA model. In the SFA the continuum electron is approximated by plane waves, thus the dipole matrix elements are calculated in the plane wave approximation (PWA).

In this Letter, we have two goals. The first is to show that electron wave packets obtained from the SFA model and from the TDSE calculation are nearly identical, but the transition dipoles calculated from PWA are significantly different from using scattering waves (SW). This result suggests a scattering wave based strong-field approximation (SW-SFA) for harmonic generation where the wave packet is derived from the SFA but the transition dipole is calculated using accurate SW. The second goal is to check whether Eq. (1) can be extended to the level of complex amplitudes such that one can relate the phases of HHG to the phases in the transition dipoles. Since phases of harmonics can be measured [12, 13], and they are needed in order to incorporate the effect of propagation in the macroscopic medium, such a study is important.

First in Fig. 1 we compare the PR cross sections of Ar, Xe and Ne calculated by treating the continuum electrons using PWA to results calculated with accurate SW's. Clearly they show significant differences. They

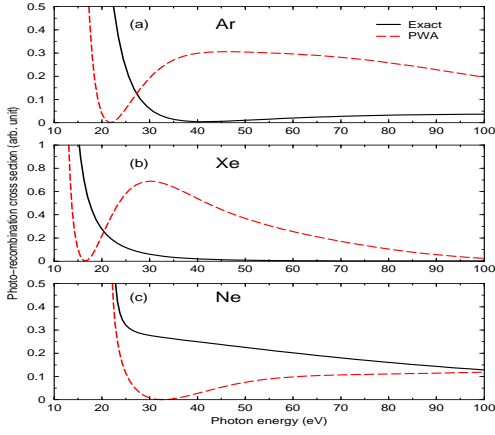


FIG. 1: (Color online) Photo-recombination cross sections of Ar (a), Xe (b) and Ne (c), obtained by using exact scattering wavefunctions (solid curves) and within the plane-wave approximation (dashed curves) for the continuum electrons.

reflect the well-known facts that plane waves are poor approximations for representing continuum electrons in atoms and molecules for energies in the energy range of tens to hundreds eV's.

To check whether the target structure affects the returning electron wave packet, in Fig. 2 we compare the wave packets  $W(E)$  for Ne deduced from the TDSE and SFA results, using Eq. (1). In the SFA case, the transition dipole is calculated within the PWA. Also shown is the  $W(E)$  obtained from scaled atomic hydrogen, with the effective nuclear charge chosen such that the ionization potential of its 1s ground state is the same as of Ne(2p). We used a laser pulse with duration (FWHM) of 10.3 fs, peak intensity of  $2 \times 10^{14}$  W/cm<sup>2</sup> and mean wavelength of 1064 nm. Note that we have normalized the results near the cut-off. The normalization is to account for the difference in the tunneling ionization rates from SFA and from TDSE, or from the different species. This comparison shows that the shape, or the energy dependence of the electron wave packets, depends only on the laser parameters.

Having established that the wave packet can be obtained from the SFA model, we now examine the accuracy of HHG calculated using the SW-SFA model where the wave packet is extracted from the SFA model and the transition dipoles are calculated using SW. In Fig. 3 we show the HHG spectra obtained from the TDSE, SFA, and SW-SFA for Ar, Xe, and Ne. For Ar and Ne, the laser pulse has peak intensity of  $2 \times 10^{14}$  W/cm<sup>2</sup> and mean wavelength of 800 nm. The laser duration (FWHM) is 10 fs for Ar and 20 fs for Ne. For Xe, the corresponding parameters are  $5 \times 10^{13}$  W/cm<sup>2</sup>, 1600 nm, and 7.8 fs, respectively. The HHG yields for Ar are shifted vertically in order to show their detailed structures. For Ne and Xe, the SFA and SW-SFA results are normalized to the TDSE results near the cutoff, i.e., close to  $3.2U_p + I_p$ ,

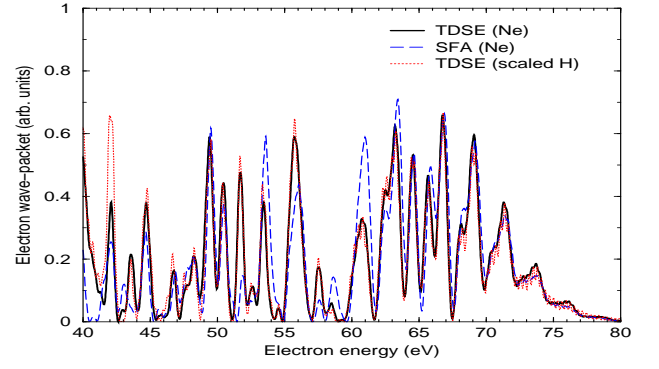


FIG. 2: (Color online) Comparison of the returning electron “wave packets” extracted from the HHG spectra of Ne, obtained by solving the TDSE (solid black line), and from the SFA model (dashed blue line). Also shown is the TDSE result for the wave packet from scaled H (dotted red line). For laser parameters, see text.

where  $U_p$  is the ponderomotive energy.

The results in Fig. 3 clearly demonstrate the good improvement of the SW-SFA over the SFA in achieving better agreement with the TDSE results. Since the SFA gives the correct wave packet, its prediction would be “reasonable” in the energy region where the dipole matrix element is rather flat, i.e., in the higher photon energy region. Thus the SFA would give adequate prediction of the HHG spectra usually near the cutoff region (after spectra are renormalized). This fact has been known [7]. The improvement of SW-SFA occurs usually at lower photon energies where the PWA for the continuum electron is grossly incorrect. In particular, the transition dipole from PWA goes through zero at some lower energies, see Fig. 1. This is the energy region where the SFA suffers the largest errors. Because of the zeros in the dipole matrix elements in the PWA, the deduced wave packets from SFA would suffer large errors at the corresponding energies. These errors are reflected as the sharp spikes in the HHG spectra calculated using the SW-SFA model.

For a realistic description of the experimental harmonic spectra, the effect of phase matching and macroscopic propagation should be addressed. To this end, the knowledge of the harmonic phase is necessary. Thus extending Eq. (1) to include the phase, can the phase of the harmonic be expressed as the sum of the phase from the wave packet and from the PR transition dipole? First we establish that there is a close relationship between the harmonics phase  $\phi$  and the PR dipole phase  $\delta$ . To be specific, we focus on Ar target. We calculated the phase difference  $\Delta\phi$  for each harmonic generated from Ar and from its scaled hydrogen (reference) partner under the same laser pulse. These calculations were carried out using the TDSE with 4-cycle and 10-cycle laser pulses, intensities of 1 and  $2 \times 10^{14}$  W/cm<sup>2</sup>, and wavelength of 1064 nm

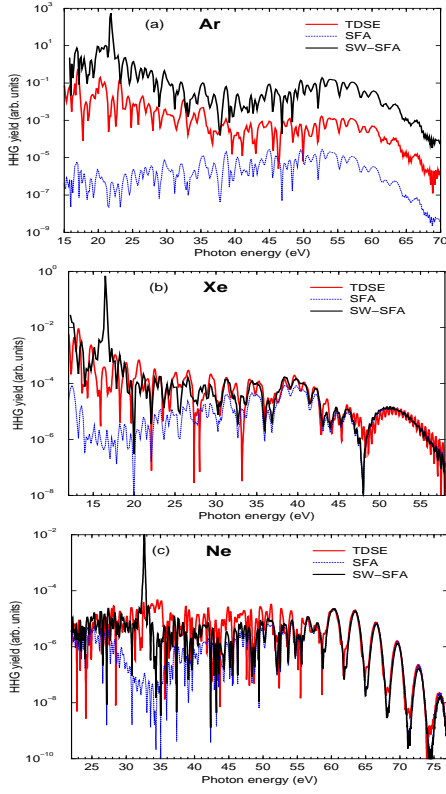


FIG. 3: (Color online) Comparison of the HHG yields obtained from numerical solution of the TDSE (solid red lines), the SFA (dashed blue lines), and the SW-SFA model (solid black lines) for Ar (a), Xe (b), and Ne (c). For laser parameters, see text.

and 800 nm. In Fig. 4(a) we compare  $\Delta\phi = \phi^{Ar} - \phi^{ref}$  with the PR dipole phase difference  $\Delta\delta = \delta^{Ar} - \delta^{ref}$ . Here we have shifted the harmonic phase difference to match the PR dipole phase difference at  $E = 60$  eV. Clearly, the two agree very well for the different lasers used. In particular, the phase jump near 40 eV (due to the Cooper minimum in Ar) is well reproduced. This indicates that the phase of the wave packets from the two systems are almost identical (up to a constant shift). Similar agreements were also found for Xe and Ne, as shown in Fig. 4(b) and (c), respectively. Here the laser pulses of 4 cycles duration are used, other parameters are given as shown in the labels. This result allows one to obtain the harmonic phase  $\phi$  from the harmonic phase of the partner atom  $\phi^{ref}$  by using  $\phi = \phi^{ref} + \Delta\delta$ .

We have also applied the same procedure by comparing the TDSE and SFA results for the same target and found that  $\Delta\tilde{\phi} = \phi^{TDSE} - \phi^{SFA}$  no longer agrees well with  $\Delta\delta = \delta^{SW} - \delta^{PW}$ . This indicates that the phase of the electron wave packet calculated from SFA differs from the one calculated by TDSE, even though their magnitudes agree well. How significant these differences affects the HHG spectra after macroscopic propagation? To this end we calculate the HHG spectra by coherently averaging

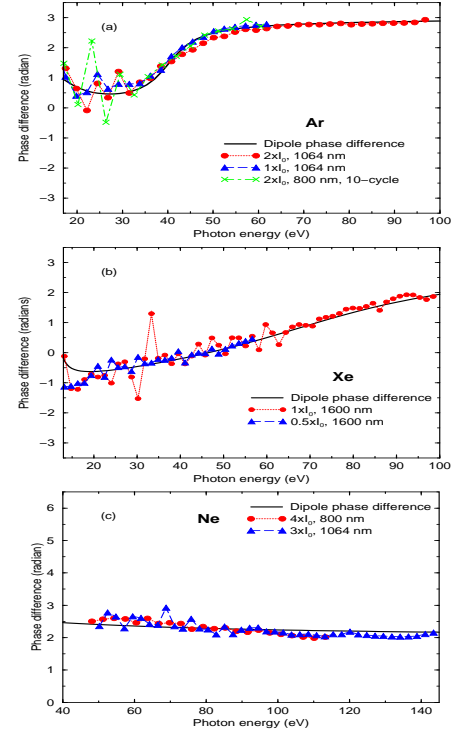


FIG. 4: (Color online) Extracted harmonic phase difference  $\Delta\phi$  between Ar and scaled hydrogen obtained with different lasers as function of emitted photon energy. The PR dipole phase difference  $\Delta\delta$  is given as solid black line. (a) Ar, (b) Xe, and (c) Ne.  $I_0 = 10^{14}$  W/cm<sup>2</sup>.

ing the induced polarization over an intensity range of the driving laser. In Fig. (5) we show the results for Ar from the TDSE, the SW-SFA, and the one with the wave packet extracted from the scaled hydrogen. All of these results are coherently averaged over 11 equally-spaced intensities in the range from  $1.8$  to  $2.2 \times 10^{14}$  W/cm<sup>2</sup>. The laser is of 800 nm wavelength and 30 fs (FWHM). The scaled H result is indeed in quite good agreement with the exact TDSE calculations. This is not surprising since we have shown that the phase of the wave packet from the scaled H and from Ar are almost identical at a single intensity. For SW-SFA, the agreement is not as good, but the improvement over SFA is still significant. The phase in SFA (or SW-SFA) can probably be improved by adding some correction to the semi-classical action, for example, as has been suggested [14, 15]. At present, it is better to extract the phase of the wave packet from the companion atomic target where TDSE calculations can be carried out.

Here we comment on the computational details. The solution of the TDSE and the choice of one-electron model potential for describing the atom have been described previously [16, 17]. The electric field of the laser pulse is written in the form  $E(t) = E_0 a(t) \cos(\omega t)$ , with the envelope given by  $a(t) = \cos^2(\pi t/\tau)$ , where  $\tau$  is 2.75

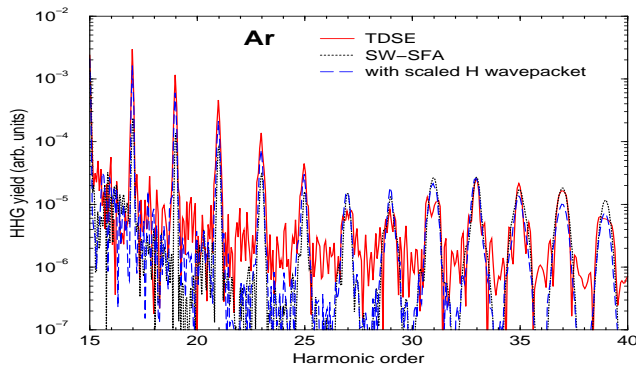


FIG. 5: (Color online) HHG spectra for Ar from the “simulated” macroscopic propagation. Shown are results from the exact TDSE (solid red line), SW-SFA (dotted black), and by using the wave packet extracted from TDSE solution for scaled H(1s) (dashed blue). For laser parameters, see text.

times the FWHM of the laser pulse. To calculate the PR cross section, the scattering wavefunction is expanded in terms of partial waves and the transition dipole is calculated for the continuum electron that has the wave vector along the polarization axis only.

Before concluding we mention several earlier related works. There exists a wealth of literature aiming at improving the SFA model, e.g., by including Coulomb distortion [14, 18], or by eikonal approximations [15]. In these approaches, the PR processes are still treated approximately. For example, use of Coulomb wave for the continuum electron would not produce the Cooper minimum in the PR cross section in Ar (see Fig. 1). The advantage of SW-SFA is that it factors out the target structure explicitly. A minimum in the HHG spectra may be attributed to the minimum in the PR cross section and this position should not change with laser parameters. Such minima are of particular interest for molecular targets since minima in the molecular dipole matrix element may be interpreted as due to the interference between the emission amplitudes from different atomic centers. Interference minima have been observed experimentally in CO<sub>2</sub> by different groups [19, 20], but the observed positions of the minimum are not identical and thus other possible interpretations have been suggested [21]. Another hot topics in recent years is the tomographic method for imaging the molecular orbitals [22]. This pioneering work deduced the dipole matrix elements of N<sub>2</sub> molecules by comparing the HHG spectra of N<sub>2</sub> vs Ar, using the factorization Eq. (1). In order to use the tomographic procedure to obtain the ground state wavefunction of N<sub>2</sub>, they approximated the continuum wavefunctions of Ar and N<sub>2</sub> by plane waves. In view of Fig. 1, their success of extracting good valence orbital wavefunction of N<sub>2</sub> is surprising. We note, however, in Itatani *et al* [22], the continuum electron energy is set equal to the photon energy, arguing that the electron re-

combining near the core should gain the additional binding energy. For Ar, this would shift the PWA curve in Fig. 1 by 15.7 eV, making the PWA result much closer to the SW result. However, this shift does not always work, see Xe and Ne examples in Fig. 1.

In conclusion, we have established quantitatively that the last step of the three-step model of HHG can indeed be expressed as the photo-recombination (PR) process of the returning electron wave packet. The wave packet depends nonlinearly on the laser, but its shape and phase are largely independent of the target. Thus if the PR of a reference target is known, the PR of another target can be derived by measuring the HHG of the two species under identical laser pulses. Since the results should be independent of the lasers, this allows for an important check on the accuracy of the measurements. We also showed that the HHG spectra can be calculated using the SW-SFA model. This model describes well the single atom HHG intensity, but the phase needs further corrections. For complex systems, SW-SFA would be a good starting point for describing the HHG spectra since the PR process is accurately incorporated. While our conclusion has been derived based on atomic targets and in the single active electron model, we anticipate that the results are applicable to molecules where accurate TDSE calculations are not available in general. The present result offers a systematic roadmap for extracting target structure information from the high-order harmonics generated by intense lasers.

This work was supported in part by the Chemical Sciences, Geosciences and Biosciences Division, Office of Basic Energy Sciences, Office of Science, U. S. Department of Energy. TM is also supported by a Grant-in-Aid for Scientific Research (C) from MEXT, Japan, by the 21st Century COE program on “Coherent Optical Science”, and by a JSPS Bilateral joint program between US and Japan.

- 
- [1] M. Drescher *et al.*, Nature (London) **419**, 803 (2002).
  - [2] T. Sekikawa *et al.*, Nature (London) **432**, 605 (2004).
  - [3] G. Sansone *et al.*, Science **314**, 443 (2006).
  - [4] R. Lopez-Martens *et al.*, Phys. Rev. Lett. **94**, 033001 (2005).
  - [5] P. B. Corkum, Phys. Rev. Lett. **71**, 1994 (1993).
  - [6] K. C. Kulander, K. J. Schafer, and J. L. Krause, in *Super Intense Laser-Atom Physics*, NATO Advanced Study Institute (Plenum Press, New York, 1993), p95.
  - [7] M. Lewenstein *et al.*, Phys. Rev. A **49**, 2117 (1994).
  - [8] Y. Mairesse *et al.*, Science **302**, 1540 (2003).
  - [9] T. Morishita *et al.*, Phys. Rev. Lett. (to appear); arXiv:0707.3157v1 [physics.atom-ph].
  - [10] J. Levesque *et al.*, Phys. Rev. Lett. **98**, 183903 (2007).
  - [11] V. H. Le, *et al.*, Phys. Rev. A **76**, 013414 (2007).
  - [12] H. Wabnitz *et al.*, Eur. Phys. J. D **40**, 305 (2006).
  - [13] T. Kanai *et al.*, Phys. Rev. Lett. **98**, 153904 (2007).

- [14] M. Yu. Ivanov, T. Brabec, and N. Burnett, Phys. Rev. A **54**, 742 (1996).
- [15] O. Smirnova, M. Spanner, and M. Ivanov, J. Phys. B **39**, S307 (2006).
- [16] Z. Chen *et al.*, Phys. Rev. A **74**, 053405 (2006).
- [17] T. Morishita *et al.*, Phys. Rev. A **75**, 023407 (2007).
- [18] J. Z. Kaminski and F. Ehlotzky, Phys. Rev. A **54**, 3678 (1996).
- [19] T. Kanai *et al.*, Nature **435**, 470 (2005).
- [20] C. Vozzi *et al.*, Phys. Rev. Lett. **95**, 153902 (2005).
- [21] A. T. Le *et al.*, Phys. Rev. A **73**, 041402(R) (2006).
- [22] J. Itatani *et al.*, Nature **432**, 867 (2004).